28 July 1995

ELSEVIER

Chemical Physics Letters 241 (1995) 345–350

CHEMICAL PHYSICS LETTERS

Light scattering from molten lithium fluoride

G.N. Papatheodorou [a,b], V. Dracopoulos [a,b]

[a] *Institute of Chemical Engineering and High Temperature Chemical Processes, University of Patras, P.O. Box 1414, 26500 Patras, Greece*
[b] *Department of Chemical Engineering, University of Patras, P.O. Box 1414, 26500 Patras, Greece*

Received 9 May 1995

Abstract

Isotropic and anisotropic light scattering (Raman) spectra of molten LiF at 865°C have been measured. The data are discussed in terms of the interaction-induced polarizability model and molecular dynamics simulations. The systematics of the reduced Raman spectra of the LiX (X = F, Cl, Br, I) melts are examined and an account of the differences is proposed in terms of the structural peculiarities of LiF.

1. Introduction

In recent years, theoretical and molecular dynamics simulation studies have been used by Madden and co-workers [1–3] to calculate the (Raman) light scattering spectra of molten NaCl, LiCl and LiF. The simulated spectra of NaCl and LiCl were in good agreement with the experimental data obtained by Raptis and co-workers [4,5] and by Giergiel et al. [6]. Due to experimental difficulties no light scattering measurements have been performed so far for molten LiF as well as for the other alkali fluoride melts. The main difficulty is the high reactivity (corrosivity) of the fluoride melts with the most commonly used optical cells made from either fused silica or sapphire.

In the work presented here we have overcome this difficulty by using a 'windowless' optical cell and we were able to measure accurately the light scattering spectra of molten LiF. The data obtained are compared with computer simulated spectra and are discussed in terms of the ion polarizability fluctuation model [1,2].

2. Experimental

Lithium fluoride was purchased from Merck Chemical Co. and was further purified by a series of slow crystallizations from the melt. Amorphous carbon containers and an inert atmosphere furnace were used for the crystallization procedures. All room temperature operations for transferring the purified salt and for filling up the optical cells were carried out in a glove box (ppm $H_2O \ll 1$) and in fused silica containers.

The windowless optical cell was made from an ultrapure graphite rod and its design was similar to that introduced by Gilbert et al. [7] for Raman spectroscopic measurements of aluminum fluoride melts. The cell consisted of an ≈ 1.5 long, 9 mm OD, 3 mm ID graphite tube closed at the bottom. Two holes of ≈ 2 mm were drilled through so as to be perpendicular to each other as well as to the axis of the tube. The excitation laser line was passed through one of these holes and the light scattered by 90° was collected through the other. The LiF amounts placed

Elsevier Science B.V.
SSDI 0009-2614(95)00641-9

into the cell were adjusted so after melting the liquid formed a droplet in the center of the cell at the level of the perpendicular holes.

By a series of trial and error experiments it was possible to adjust the size of the droplet so as to stay at the center of the cell without spilling off through the open holes any excess of melt. After filling the cell with LiF, and before melting, the cell was placed and sealed in a fused silica protective tube (12 mm OD, 9 mm ID) under ≈ 0.8 atm of pure Ar gas.

The Raman spectroscopic system and the high temperature optical furnace used were the same as before [8]. A constant power of 400 mW of the 488.0 nm laser line was used to excite the spectra. The spectral slit width was ≈ 2 cm^{-1} and the VV and HV configurations were measured from 3 to 600 cm^{-1}. At around 550 cm^{-1} the scattered light for both configurations was practically zero. The spectrometer was interfaced with a PC for recording the spectra, for calculating isotropic intensities, reduced intensities and depolarization ratios and for statistically smoothing the spectra.

3. Results and discussion

The VV and HV spectra of LiF were measured 20°C above its melting point (m.p. = 845°C). In terms of the measured polarizations at different wavenumbers (ω) the isotropic and anisotropic intensities were calculated from the relations

$$I_{\mathrm{ISO}}(\omega) = I_{\mathrm{VV}}(\omega) - \tfrac{4}{3} I_{\mathrm{HV}}(\omega),$$
$$I_{\mathrm{ANISO}}(\omega) = I_{\mathrm{HV}}(\omega). \qquad (1)$$

Fig. 1 shows the raw scattering data of $I_{\mathrm{VV}}(\omega)$ and $I_{\mathrm{ANISO}}(\omega)$ ($I_{\mathrm{HV}}(\omega)$) as well as the calculated $I_{\mathrm{ISO}}(\omega)$. The reduced Raman intensity [9,10], $R_\sigma(\omega)$, shown as an insert in Fig. 1, is related to the intensity $I_\sigma(\omega)$,

$$R_\sigma(\omega) = I_\sigma(\omega)\,\omega(\omega_0 - \omega)^{-4}[n(\omega)+1]^{-1}, \qquad (2)$$

where ω_0 is the laser excitation wavenumber, $n(\omega) + 1 = [\exp(h\omega c/kT) - 1]^{-1} + 1$ is the Boltzmann thermal population factor and σ stands for either ISO or ANISO. The anisotropic intensity is rather

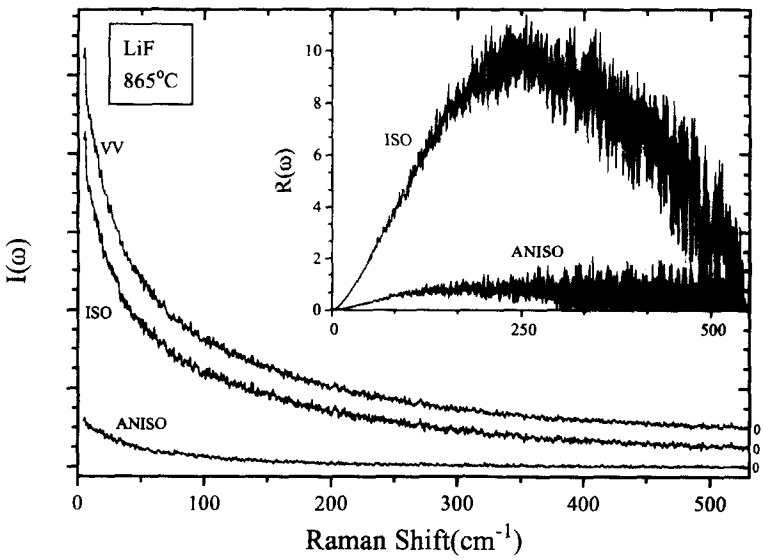

Fig. 1. Relative scattering intensities for the VV, ISO and ANISO(HV) configurations. Laser line 488.0 mm; laser power 400 mW; spectral slit width ≈ 2 cm^{-1}; time constant 0.3 s; ordinate maximum scale ≈ 3000 counts/s. Insert: reduced spectra for the ISO and ANISO configuration.

weak and the spectra are strongly polarized. The maximum of $R_{ISO}(\omega)$ occurs at $\omega_{max} \approx 240$ cm^{-1} and in the overall frequency region $R_{ISO}(\omega) \gg R_{ANISO}(\omega)$. The mechanism for light scattering from alkali halides is related to the fluctuation of the polarizability tensor $\Delta\Pi$ [1]. The spectra are determined by the time-dependent correlation function

$$I_\sigma(\omega) \propto \int_0^\infty \mathrm{d}t\, \mathrm{e}^{-\mathrm{i}\omega t}\langle \Delta\Pi_\sigma(t) \cdot \Delta\Pi_\sigma(0)\rangle, \quad (3)$$

where depending on σ the polarizability fluctuations are expressed as

$$\Delta\Pi_{ISO} = \Pi^{SR}_{ISO} + \Pi^{\gamma}_{ISO}, \quad (4)$$

$$\Delta\Pi_{ANISO} = \Pi^{SR}_{ANISO} + \Pi^{DID}_{ANISO} + \Pi^{B}_{ANISO} + \Pi^{\gamma}_{ANISO}. \quad (5)$$

The Π^i_σ terms refer to different fluctuation mechanisms; Π^{SR}, a short-range term, describes the effect of near-neighbour interactions on the ionic charge clouds, Π^{DID} is the dipole–induced-dipole term, Π^B and Π^γ give the changes in polarizability induced on a given ion by the Coulomb field gradient and the Coulomb field, respectively.

The separate contribution of the Π^{SR} and Π^γ terms to the isotropic light scattering intensity of LiF have been calculated by Madden [1]. The relative intensities I^{SR}_{ISO} and I^{γ}_{ISO} are comparable while the cross term $\Pi^{SR}_{ISO} \cdot \Pi^{\gamma}_{ISO}$ has practically no effect on the overall isotropic intensivity. A comparison of the simulated and experimental isotopic spectra is given in Fig. 2. By matching the theoretical intensity at 10 cm^{-1} to the experimental value at the same wavenumber the overall spectra can be compared. A remarkable agreement exists between the experimental and the simulated spectra.

The contributions of the different terms of Eq. (5) to the anisotropic scattering intensity have also been calculated by Madden [1]. Due to the small polarizabilities of both Li^+ ($\alpha_{Li^+} = 0.03$ Å^3) and F^- ($\alpha_{F^-} \approx 0.7$ Å^3) the DID mechanism does not contribute much to the intensity. The Π^{SR} and Π^B terms are shown to give the largest contributions, but cancella-

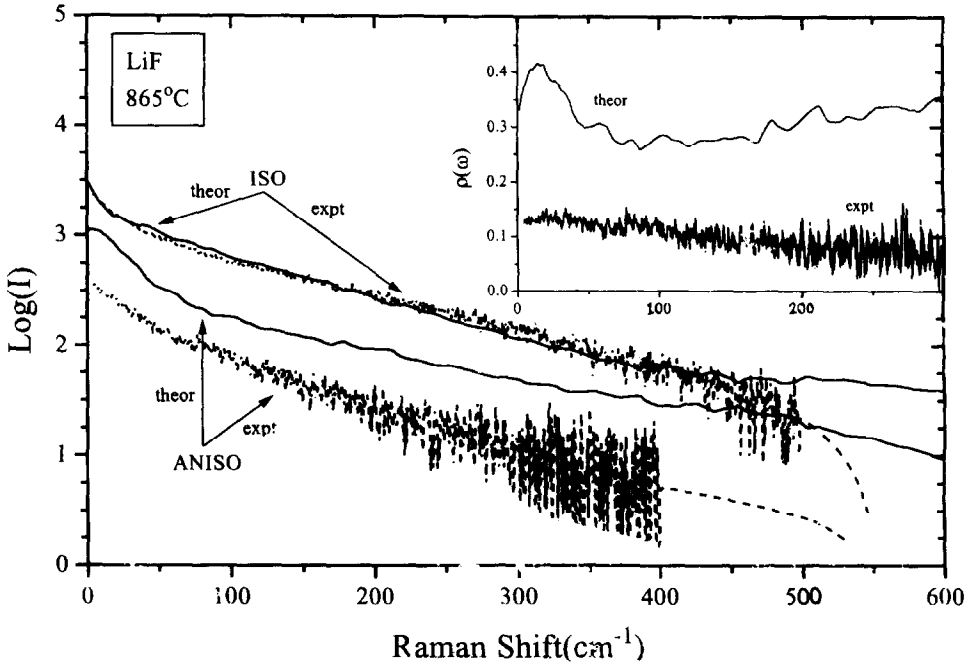

Fig. 2. Comparison of the logarithmic experimental relative intensities with the simulated [1] spectra of LiF. At high frequencies the experimental $I(\omega)$ tends to zero and the apparent noise in the log I plot increases; dashed lines show the statistically averaged experimental log I at large ω. Insert: experimental and simulated depolarization ratios of LiF.

tion effects due to SR/B cross correlation drastically lower the overall intensity. A comparison between the theoretical and experimental anisotropic intensity is given in Fig. 2. It seems that the variation (slope) of log I with wavenumber is predicted relatively accurately but the theoretical overall anisotropic intensity is overestimated. The differences are emphasized in the insert of Fig. 2 where the experimental and theoretical depolarization ratios

$$\varrho(\omega) = I_{\mathrm{ANISO}}(\omega)/I_{\mathrm{ISO}}(\omega) + \tfrac{4}{3} I_{\mathrm{ANISO}}(\omega) \qquad (6)$$

are compared. The experimental $\varrho(\omega)$ is essentially constant and close to 0.1 which indicates that $I_{\mathrm{ANISO}}(\omega)$ is weak and approximately proportional to $I_{\mathrm{ISO}}(\omega)$. Since the latter is dominated by short-range interactions, it appears that the anisotropic light scattering intensity also probes short-range interactions. The long-range field gradient term Π^B is efficiently screened [2] and only nearest-neighbour ions make contributions to the polarizability fluctuations. Thus, Π^B and Π^{SR} reflect short-range interactions and probably both contribute to the weak anisotropic scattering intensity.

The $\omega_{\max}$ of the reduced spectra of LiF does not follow the systematics established by the spectra of the other three lithium halide melts. This is shown in Fig. 3 where the $R_{\mathrm{ISO}}(\omega)$ spectra of LiX (X = Cl, Br, I) [11,12] and LiF are presented together. With the exception of LiF having one maximum the other salts show a well-defined shoulder band (ω_2) and a band maximum (ω_1). A close examination of the spectra reveals that the intensity of the ω_2 band relative to the ω_1 band increases from I to Br to Cl. The systematics lead to the conclusion that in LiF the ω_2 is the predominant band with a maximum at 240 cm^{-1} while the ω_1 band has a weak intensity which probably hides at the high wavenumber tail of the spectra (400–500 cm^{-1}).

Raptis and co-workers, in their extensive studies of all molten alkali halides (except fluorides), have shown [4,5,13] that the $\omega_{\max}$ in the reduced spectra is close to the Debye frequency (ω_{D}) of the corre-

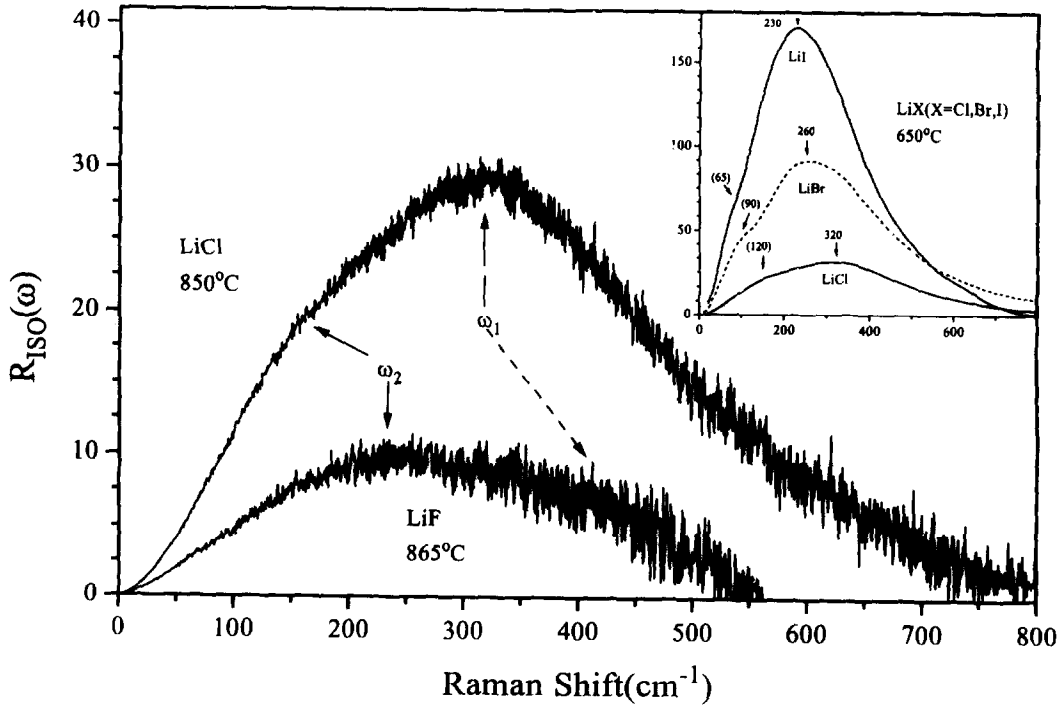

Fig. 3. Reduced isotropic spectra of LiCl(850°C) taken from Ref. [12] and of LiF(865°C) taken from Fig. 1; ordinate values are arbitrary. Insert: reduced isotropic spectra of LiX (X = Cl, Br, I) at 650°C taken from Ref. [11]; ordinate values indicate relative intensities.

Table 1
Debye frequencies (ω_D) of crystalline lithium halides and observed frequencies (ω_1, ω_2) in the reduced Raman spectra of the corresponding melts (in cm^{-1})

	LiI	LiBr	LiCl	LiF
ω_D [a]	195	238	292	(450) [c]
ω_1 [b]	230	260	320	(400–500) [d]
ω_2 [b]	(65)	(90)	(120)	240 [d]

[a] Ref. [14].
[b] Values for isotropic spectra [11].
[c] Number in parentheses indicates shoulder band.
[d] This work.

sponding solid. Table 1 gives the values of ω_D, ω_2 and ω_1 for the four lithium halide salts. The trends in the table suggest that for LiF the ω_1 frequency is expected to be close to ω_D, i.e. in the 400–500 cm^{-1} region; this supports the above assignment which associates the ω_{max} for LiF with the ω_2 band, seen as a shoulder band in the other lithium halides. A possible account of the spectral differences between LiF and LiX (X = Cl, Br, I) may lie in the structural peculiarities imposed in the melt by the relative sizes of the Li^+ and X^- ions. In LiCl, LiBr and LiI melts the X^- anions are in contact with each other having the Li^+ cation 'enclosed' in the voids created by the anions. Even for LiCl having the largest r_{Li^+}/r_{X^-} (X = Cl, Br, I) ratio, the neutron diffraction data [15] indicate a tetrahedral coordination with ionic distances allowing Cl^-–Cl^- contact. In contrast, the relative sizes of the Li^+ and F^- ions ($r_{Li^+}/r_{F^-} \approx 0.75$) do not allow anion–anion contact for either fourfold or sixfold coordination. These structural limitations imply that in LiCl, LiBr and LiI melts polarizability fluctuations induced on a given X^- arise from both the Li^+ and X^- interactions and can be associated with the two bands (ω_1, ω_2) observed in the $R_{ISO}(\omega)$ spectra. For the LiF melt the fluctuations of the F^- polarizability are predominately induced by the Li^+ cations in contact with the anion; this presumably is reflected in the appearance of only one band in the reduced spectra.

An alternative interpretation of the origin of the ω_1 and ω_2 bands could be based on the distinct contributions of the different fluctuation mechanisms to the spectra. A correspondence between the two terms in Eq. (4) and the two bands of the isotropic spectra in Figs. 1 and 3 could be anticipated. For the LiX (X = Cl, Br, I) melts having a soft halide anion the short-range overlap interactions predominate the spectra with an ω_1 band at higher energies than the ω_2 band which is associated with the Coulomb field term; in support of this assignment are the relative intensities for the two bands which are in agreement with the simulated spectra of LiCl where $I^{SR}_{ISO} \approx 3I^{\gamma}_{ISO}$ [1]. On the other hand, the electrons of the F^- anion are more localized and the Coulomb interactions between the two small and 'hard' Li^+ and F^- ions diminish the SR-overlap interactions. Thus, the main band (ω_2) seen in the LiF reduced spectra originates from the Π^{γ} term.

Finally, it should be pointed out that molecular dynamics studies of the dynamic structure factors of molten LiCl [2,3,16,17] have predicted the presence of optical modes in the melt. The power spectra of the velocity autocorrelation function [16,17] and the calculated phonon density of states [17] show two optical modes at wavenumbers between ≈ 100 and ≈ 450 cm^{-1} which are in the range of the experimentally measured bands in the reduced spectra of LiCl. Similar calculations for molten LiF would be useful in understanding the origin of the ω_1 and ω_2 bands in the lithium halide melts.

Acknowledgement

This work was supported by the EU Human Capital and Mobility program. We thank Dr. E.A. Pavlatou for helping with the experiments.

References

[1] P.A. Madden, K.F. O'Sullivan, J.A.B. Board and P.W. Fowler, J. Chem. Phys. 94 (1991) 918.
[2] P.A. Madden and K.F. O'Sullivan, J. Chem. Phys. 95 (1991) 1980.
[3] K.F. O'Sullivan and P.A. Madden, J. Phys. Condens. Matter 3 (1991) 8751.
[4] C. Raptis, R.A.J. Bunten and E.W.J. Mitchell, J. Phys. C 16 (1983) 5351.
[5] E.W.J. Mitchell and C. Raptis, J. Phys. C 16 (1983) 2973.
[6] G. Giergiel, K.R. Subbaswamy and P.C. Eklund, Phys. Rev. B 29 (1984) 3490.
[7] B. Gilbert, G. Mamantov and G.M. Begun, J. Chem. Phys. 62 (1975) 950.

[8] S. Boghosian and G.N. Papatheodorou, J. Phys. Chem. 93 (1989) 415.
[9] M. Brooker and G.N. Papatheodorou, in: Advanvces in molten salt chemistry, Vol. 5, eds. G. Mamantov and C.B. Mamantov (Elsevier, Amsterdam, 1983) p. 27.
[10] O. Faurskov Nielsen, Ann. Rep. Prog. Chem. Sect. C, Phys. Chem. 91 (1994) 3, and references therein.
[11] S.G. Kalogrianitis, T.G. Michopoulos, E.A. Pavlatou and G.N. Papatheodorou, Proc. 9th Int. Symp. Molten Salts, Vol. 94-13 eds. C.L. Hussey, D.S. Newman, G. Mamantov and Y. Ito (The Electrochem. Soc., 1994) p. 284.
[12] G.N. Papatheodorou, S.G. Kalogrianitis, T.G. Michopoulos and E.A. Pavlatou, Isotropic and Anisotropic Raman Scattering from Molten CsCl–LiCl Mixtures: Composition and Temperature Effects, submitted for publication.
[13] C. Raptis and R.L. McGreevy, J. Phys. Condens. Matter 4 (1992) 5471, and references therein.
[14] J.R. Hardy and A.M. Karo, The lattice dynamics and statics of alkali halide crystals (Plenun Press, New York, 1979).
[15] M.A. Howe and R.L. McGreevy, Philos. Mag. B 58 (1988) 485.
[16] S. Okazaki, Y. Miyamot and I. Okada, Phys. Rev. B 45 (1992) 2055.
[17] K. Kinugawa, J. Chem. Phys. 97 (1992) 8581.